New BIOTECHNOLOGY 66 (2022) 8–15

Contents lists available at ScienceDirect

New BIOTECHNOLOGY

journal homepage: www.elsevier.com/locate/nbt

Full length Article

The impact of biomass withdrawal strategy on the biomass selection and polyhydroxyalkanoates accumulation of mixed microbial cultures

Rafaela A.P. Cruz [a,b], Adrian Oehmen [c], Maria A.M. Reis [a,b,*]

[a] UCIBIO – Applied Molecular Biosciences Unit, Department of Chemistry, School of Science and Technology, NOVA University Lisbon, 2819-516 Caparica, Portugal
[b] Associate Laboratory i4HB - Institute for Health and Bioeconomy, School of Science and Technology, NOVA University Lisbon, 2819-516 Caparica, Portugal
[c] School of Chemical Engineering, The University of Queensland, St Lucia, Queensland, 4072, Australia

ARTICLE INFO

Keywords:
Polyhydroxyalkanoates (PHA)
Mixed microbial cultures (MMC)
Biomass withdrawal
Process optimization
Sequencing batch reactors (SBR)
Bioplastics

ABSTRACT

The production of polyhydroxyalkanoates (PHA) by mixed microbial cultures (MMC) has been studied as an alternative to pure cultures in order to reduce the price of PHA through use of open systems and low-cost substrates, such as agro-industrial sub-products. However, the widespread applicability of this process depends on the optimization of operational factors impacting PHA productivity. This study addresses the impact of biomass withdrawal strategy on the performance of MMC selection reactors and consequently on biomass productivity and global PHA productivity. Two selection reactors were operated in parallel under similar conditions, except for the timing of biomass withdrawal, at the end of the famine phase (Reactor 1, R1) versus at the end of the feast phase (Reactor 2, R2) at an organic loading rate of 100 Cmmol.L^{-1}.d^{-1} and solids retention time of 4 days. The biomass selected in both conditions had similar PHA storing capacity as shown by the similar yields of PHA per substrate obtained in the accumulation assays; however, R1 reached a higher biomass productivity (about 4-fold higher than R2). This study demonstrated that removing the excess biomass at the end of the famine phase resulted in a much higher global PHA productivity and that the key parameter affecting the global PHA productivity of the 2-stage system was the volumetric biomass productivity. Results obtained provide important insight into how MMC systems can be best operated to maximize PHA productivity.

Introduction

Polyhydroxyalkanoates (PHA) are biodegradable polymers, accumulated as intracellular reserves by numerous microorganisms, with physico-chemical properties similar to those of commonly used petrochemical polymers [1]. It has been proposed that the use of conventional plastics should be replaced by alternatives such as PHA in broad single-use utilizations such as food packaging (films, utensils, foam trays), agriculture (mulch film) and hygiene (flushable products) [2]. PHA can be produced by pure cultures (e.g, recombinant *Escherichia coli*, *Cupriavidus necator*) or mixed microbial cultures (MMC). While the former focuses on obtaining an axenic culture, which entails significant costs of sterilization and the utilization of refined carbon substrates (40–50 % of the total production costs), MMC are based on the principle of natural selection and do not require sterile conditions (cheaper equipment and less energy) resulting in lower investment and operational costs [3,4]. In addition, wastes/by-products can be used [5–13], reducing the feedstock costs and allowing the integration of the PHA production process within the circular bioeconomy concept [14,15].

The typical process for the production of PHA by MMC includes three stages: acidogenic fermentation, culture selection and PHA accumulation, which has been applied by multiple research groups using various feedstocks [10,16,17]. The acidogenic fermentation stage converts organic waste substrates into a mixture of volatile fatty acids (VFA), and

Abbreviations: DO, dissolved oxygen; F/F, feast to famine ratio; F/M, Food to Microorganism; f_{PHA}, ratio of PHA to active biomass; 3HB, 3-hydroxybutyrate; HRT, hydraulic retention time; 3HV, 3-hydroxyvalerate; k, PHA degradation rate constant; MMC, mixed microbial cultures; OLR, organic load rate; P(3HB-co-3HV), poly (3-hydroxybutyrate-co-3-hydroxyvalerate); $Prod_{PHA}$, PHA volumetric productivity; $Prod_X$, biomass volumetric productivity; qPHA, specific PHA storage rate; -qS, specific substrate uptake rate; SBR, sequential batch reactor; SRT, solids retention time; TSS, total suspended solids; VFA, volatile fatty acids; VSS, volatile suspended solids; X_A, active biomass; X_f, amount of biomass final; X_i, amount of biomass initial; $Y_{PHA/S}$, PHA storage yield; $Y_{X/PHA}$, growth yield on PHA; ΔX, amount of biomass produced.

* Corresponding author.
E-mail address: amr@fct.unl.pt (M.A.M. Reis).

https://doi.org/10.1016/j.nbt.2021.08.004
Received 14 June 2021; Received in revised form 18 August 2021; Accepted 20 August 2021
Available online 24 August 2021

possibly lactate and ethanol, which are precursors of PHA biosynthesis. The culture selection stage aims at enriching MMC in PHA-producing bacteria by subjecting the culture to transient conditions of carbon availability – known as the feast and famine regime – using the VFA-rich stream from the fermentation stage. The PHA accumulation stage consists of feeding a fraction of the enriched culture with excess VFA under growth limiting conditions until the maximum accumulation potential of the culture is reached [18,19].

A key step in designing a PHA production process using MMC is the selection of a robust culture, while maximizing the enrichment of microorganisms with high PHA storage capacity, as illustrated in several studies [5,18,19]. The selective pressure to achieve a high PHA-producing population typically involves alternating excess (feast) and limitation (famine) of external organic carbon substrate, usually in a sequencing batch reactor (SBR). Feast and famine conditions enforce environmental selective pressure by making PHA-storing and non-PHA storing populations compete for the external organic substrate that is only available during the feast phase, and by giving environmental advantage to PHA-storing microorganisms during the longer famine phase, since only they can survive by oxidizing the stored PHA to obtain carbon and energy necessary for growth and maintenance. Furthermore, when using nutrient-deficient feedstocks (e.g, fruit pulp and cheese whey), a double growth limitation strategy can be applied by uncoupling the carbon and the nitrogen feeding in order to further grant competitive advantage to PHA-storing bacteria [6]. Several authors have found that this strategy selects for a culture with high PHA storage yield and cell growth rate, while maintaining culture stability, even when imposing high organic loading rates (OLR), leading to increased PHA volumetric productivity [6,20–22].

The SBR is the most frequently used configuration for selecting an MMC for the production of PHA, due to the simplicity of operation and the ability to modify the process parameters easily [19,23]. In typical SBR operation, the biomass withdrawal phase is set at the end of the famine phase and before the settling phase [24–27]. In this case, PHA-storing bacteria grow on the internal PHA reserves during the long famine phase. This withdrawn biomass, usually with a low percentage of internal PHA due to the period of organic carbon starvation, is then used to inoculate a reactor for PHA production. In recent years, it has been suggested that removing the surplus biomass from the selection reactor at the end of the feast phase, [20–22], when cells have already accumulated a significant amount of PHA, can reduce the length of the accumulation assays needed for PHA production. Despite the potential for reducing the costs of operation, the impact of this strategy on the biomass concentration and global PHA productivity is still unclear, since the fraction of biomass that is purged at the end of the feast phase does not grow during the famine phase, contrary to the traditional procedure of biomass withdrawal at the end of the famine. Indeed, further work is needed to establish if the reduced time needed during the accumulation stage resulting from biomass withdrawn at the end of the feast phase compensates for the reduced biomass production as compared to biomass withdrawn at the end of the famine phase, which motivated the present study. To date, it appears that no studies have been reported comparing these two different PHA production strategies, thus the true impact of this operational change on overall PHA productivity is unknown.

This study aimed to elucidate the effect of two different biomass withdrawal strategies on the performance of MMC biomass selection, and consequently, on biomass productivity and global PHA productivity. For this purpose, uncoupled carbon and nitrogen feeding was applied to two parallel SBRs fed with a synthetic mixture of acetic and propionic acids to assure a constant composition of the feed and eliminate any possible interference by the variability of the substrate composition. The potential for PHA accumulation by the cultures selected under the two strategies was assessed in accumulation assays and the global PHA productivity of both systems was compared, in order to understand the operational strategies that enhance PHA production efficiency in MMC.

Materials and methods

Culture selection stage

Two similar SBRs with working volumes of 2 L were operated under the feast and famine regime with the uncoupled ammonia feeding strategy (i.e. ammonia was fed after the carbon source was depleted from the medium, corresponding to the beginning of the famine phase) to select a culture with high PHA accumulation capacity. The same conditions were applied to both reactors, except for the moment of biomass purging: biomass was withdrawn from Reactor 1 (R1) at the end of the famine phase, while in Reactor 2 (R2) the biomass was withdrawn at the end of the feast phase. The reactors were inoculated with activated sludge from the municipal wastewater treatment plant of Mutela, Almada, Portugal. The sludge was aerated for approximately 6 h prior to reactor inoculation, and the initial total/suspended solids (TSS/VSS) concentration was 2.78 ± 0.00 g $TSS.L^{-1}$ and 2.29 ± 0.12 g $VSS.L^{-1}$ in R1 and 2.85 ± 0.04 g $TSS.L^{-1}$ and 2.34 ± 0.02 g $VSS.L^{-1}$ in R2.

Each SBR cycle consisted of a reaction phase of 11 h, followed by settling (45 min) and withdrawal (15 min) phases. In the reaction phase, the carbon source was fed during the first 2.5 min, the nitrogen source was added after the end of the feast phase (varying between 60 to 280 min), while the biomass was withdrawn after 645 min in R1 and before the addition of the nitrogen source in R2. During the withdrawal phase, half the volume of the reactors was discharged and replaced with fresh feeding solution at the beginning of the next cycle, resulting in a hydraulic retention time (HRT) of 1 d. For both reactors, a volume of 250 mL per cycle was withdrawn, maintaining a solids retention time (SRT) of 4 days. The carbon feeding solution contained per L: 100 Cmmol of VFA, consisting of 80 % acetic acid and 20 % propionic acid on a Cmol basis, 600 mg $MgSO_4.7H_2O$, 70 mg $CaCl_2.2H_2O$, 10 mg allyl-N thiourea (to prevent nitrification), 100 mg ethylene-diaminetetraacetic (EDTA), and 2 mL of a micronutrients solution described by [28], and the pH was adjusted to 7.2–7.3 with 5 M NaOH. The carbon source composition was chosen accordingly to the literature [20,21,29], so that a copolymer of 3-hydroxybutyrate (3HB) and 3-hydroxyvalerate (3HV) with an approximate content of 80:20 %Cmol 3HB:3HV could be obtained, as its properties are considered to be more flexible than those of pure poly (3HB) and suitable for many applications including packaging [2,30]. A nutrient solution composed of NH_4Cl, KH_2PO_4, K_2HPO_4 was prepared to correspond to a C:N:P ratio of 100:7:1 (Cmol basis) and added at the beginning of the famine phase. Due to the difference in reactor volume in the famine phase caused by the biomass withdrawal in R2, 25 mL of nutrient solution was added in R1 and 250 mL was added in R2. After day 36 of reactor operation, a phosphate buffer composed by 0.1 M KH_2PO_4 and 0.1 M K_2HPO_4 was included in the carbon feeding solution in order to stabilize the high pH variation occurring during the feast phase, which was leading to the addition of high amounts of NaCl and HCl by the pH control system. Thus, after day 36, the nutrient solution was adjusted to include only NH_4Cl to achieve a C:N ratio of 100:7 (Cmol basis).

The temperature of both SBRs was controlled at 22 ± 1 °C using a thermostat bath and pH was controlled at 7.5 ± 0.2 by automatic addition of 1 M HCl and 0.5 M NaOH as needed. Air was supplied by an air compressor through a silicone tube disperser inside the reactors, where dissolved oxygen (DO) levels were maintained above 2 $mg.L^{-1}$ by adjusting the air flow rate. DO concentration and pH were measured online using analog sensors (Mettler Toledo, LLC, Columbus, OH, USA). Stirring (250 rpm) was performed with a stainless steel shaft with two impellers: a 6-bladed Rushton disc turbine and a 3-bladed pitched blade impeller (bbi-biotech GmbH, Berlin, Germany).

Each SBR was closely monitored weekly by collecting samples during the full length of the reaction phase. Samples were analysed for TSS and VSS, VFA and PHA according to the analytical methods described below.

PHA accumulation assays

Fed-batch assays were performed in order to evaluate the maximum accumulation capacity of the cultures selected in both SBRs. PHA accumulation assays were performed in a BioFlo®/CelliGen® 115 system (Eppendorf AG, Germany) with 1 L working volume glass vessel and controlled air flow and agitation (3.0 $L.min^{-1}$ and 250 rpm respectively) using 500 mL of surplus biomass from each culture selection SBR. Sludge from R1 was collected at the end of the famine phase and sludge from R2 was collected at the end of the feast phase. pH was controlled at 7.5 ± 0.2 by automatic addition of 0.5 M HCl.

The PHA accumulation assays were performed using a pulse-wise strategy, maintaining the same Food to Microorganism (F/M) ratio as in the selection reactors, where the carbon addition was corrected for the volume of samples taken during the tests. The carbon source solution used had the same composition as that fed to the selection reactors (80 % acetic acid and 20 % propionic acid on a Cmol basis). The accumulation assays were maintained until the reaction was considered to have slowed down significantly (DO levels reaching 80 % of saturation, usually 8−10 h of reaction time). Samples were collected over the full duration of the accumulation assays in order to follow the VFA consumption and the PHA content.

Analytical methods

Samples were collected over the duration of the SBR cycles and accumulation assays and immediately centrifuged at 9600 rcf for 3 min. The supernatant was filtered through 0.45 μm membrane filters (Whatman®, Cytiva, Marlborough, MA, USA) and the pellets were lyophilized. Samples for determination of TSS and VSS were treated according to standard methods [31]. VFA concentrations were determined by high-performance liquid chromatography as described by [6]. Soluble ammonia and phosphate concentrations were quantified by a segmented continuous flow analyser (Skalar San++ automated system, Skalar Analytical B.V, Breda, The Netherlands). Lyophilized pellets were used to quantify PHA by gas chromatography with flame ionization detector (Bruker 430-GC, Bruker, MA, USA) according to the method described by [32]. The concentrations of monomers 3HB and 3HV were calibrated through standard curves with a copolymer P(3HB-co-3HV) (88:12 %mol 3HB:3HV) and heptadecane (Sigma-Aldrich, St. Louis, MO, USA) as internal standard (concentration of approximately 1000 $mg.L^{-1}$).

Microbial population analysis

Biomass samples were collected from the initial inoculum and from the selection reactors during the operational steady states and were analysed by high-throughput sequencing. DNA extraction (using the FastDNA Spin kit for Soil (MP Biomedicals, Santa Ana, CA, USA)), library preparation (custom protocol based on [33]), 16S V1-3 rRNA gene amplicon sequencing on a MiSeq System (Illumina, Inc., San Diego, CA, USA) following the standard guidelines, and bioinformatic processing were carried out by DNASense (http://dnasense.dk/), Aalborg, Denmark.

The biomass samples were also observed with Nile Blue staining using an Olympus BX51 epifluorescence microscope (Olympus Europa SE & Co. KG, Hamburg, Germany) at a magnification of 1000 × . Samples were prepared by adding 50 μL of a 0.2 % aqueous solution of Nile Blue A (Sigma-Aldrich) to 1 mL of fresh biomass collected from the reactor at the end of the feast phase and placed at 55 °C for 10 min in a water bath. A drop of the sample was then transferred to a glass slide, covered with a coverslip and examined under the microscope.

Calculations

The feast to famine ratio (F/F) was calculated by dividing the length of the feast phase by the length of the famine phase. The end of the feast phase was identified by the observation of a sharp rise of the DO concentration, indicating the moment of carbon source exhaustion.

Active biomass concentration (X_A, $g.L^{-1}$) was calculated by subtracting PHA concentration ($g.L^{-1}$) from VSS concentration ($g.L^{-1}$). The generic chemical formula of biomass $C_5H_7NO_2$ was used to express the X_A in Cmol (22.6 $g.Cmol^{-1}$). The PHA content in the biomass was determined in terms of percentage of TSS (wt. basis).

VFA concentration corresponds to the sum of acetic and propionic acid concentrations in the medium at a given time and PHA concentration equals the sum of 3HB and 3HV, both in $Cmmol.L^{-1}$. Specific substrate consumption rate ($-q_S$, $Cmol\text{-}S.Cmol\text{-}X_A^{-1}.L^{-1}$) and specific PHA accumulation rate (q_{PHA}, $Cmol\text{-}PHA.Cmol\text{-}X_A^{-1}.L^{-1}$) were calculated by dividing the slope of the linear regression of the experimental data of VFA and PHA concentration over time, respectively, by the average X_A concentration during the feast phase.

The yield of PHA per substrate ($Y_{PHA/S}$, $Cmol\text{-}PHA.Cmol\text{-}S^{-1}$) was calculated by dividing total amount of PHA produced by the total amount of VFA consumed. The volumetric PHA production rate (r_{PHA}, $g\text{-}PHA.L^{-1}.h^{-1}$) was calculated by dividing the concentration of PHA produced by the time elapsed. The yield of biomass per PHA ($Y_{X/PHA}$, $Cmol\text{-}X_A.Cmol\text{-}PHA^{-1}$) was calculated by dividing the total amount of X_A produced by the total amount of PHA consumed during the famine phase. The PHA degradation rate constant (k) was calculated using the expression proposed by [34]. The volumetric biomass productivity ($Prod_X$, $g\text{-}X_A.L^{-1}.d^{-1}$) was defined by dividing the average X_A ($g.L^{-1}$) during the period of operation considered by the SRT (d).

For the PHA accumulation assays, the PHA produced and the VFA consumed, converted to Cmmol, were plotted over the time of each accumulation assay (data not shown). Polynomial functions (quadratic, correlation coefficient above 0.9) were adjusted to the results in order to calculate the maximum PHA produced, the VFA consumed at that point and the time elapsed. A threshold of 90 % of the maximum PHA produced was considered to normalize the results obtained and compare the overall accumulation performance of the biomass from the different SBRs that were used in the accumulation assays. The time necessary to reach 90 % of the total PHA produced was assessed and the overall $Y_{PHA/S}$ and r_{PHA} were calculated as previously described for each reactor. In addition, $-q_S^{max}$, q_{PHA}^{max}, $Y_{PHA/S}^{max}$ and r_{PHA}^{max} were calculated as described above for the periods in which the biomass presented maximum activity (highest kinetic rates), namely, each of the first three pulses of accumulation assays using biomass from R1, and the first pulse of accumulation assays using biomass from R2.

The global PHA productivity was calculated by multiplying the volumetric biomass productivity by the cycle length and the maximum PHA content of the accumulation assays divided by the time elapsed.

Single factor ANOVA was used to establish differences in means using Minitab software, with significance declared at a confidence level of 95 %.

Results and discussion

Selection reactors

The performance observed during culture enrichment for both reactors was regularly assessed, where it was assumed that the reactors were at pseudo-steady state when the concentration of biomass, the F/F and the %PHA at the end of the feast phase were each stable (Figures A1 and A2 in Supplementary material Appendix A). The kinetic parameters were calculated using data from the cycles monitored during that period, which corresponded to days 150–185 in R1 and to days 165–200 in R2.

Fig. 1 illustrates the behaviour of the selected MMC during one SBR cycle of both reactors, during the stable operational period, where the profiles of VFA, PHA, X_A and ammonia are shown for R1 (a) and R2 (b). During the feast phase, the VFA solution was fed at the beginning of the

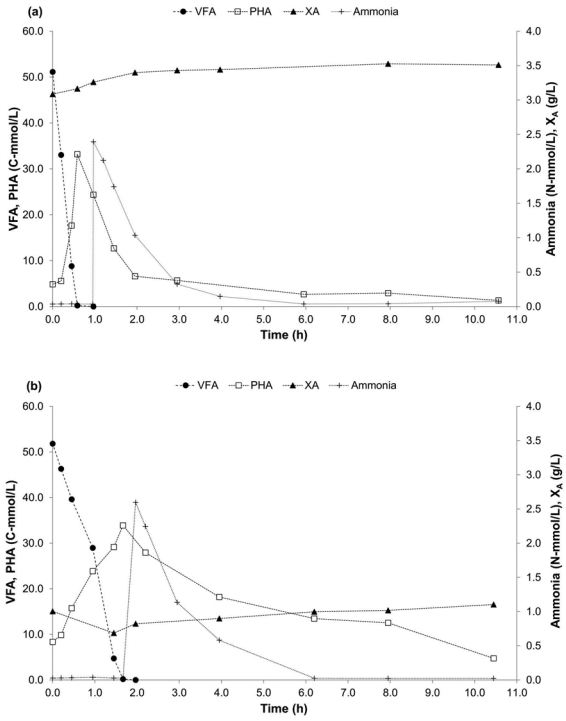

Fig. 1. Concentration profiles of VFA, PHA, X_A and ammonia during a typical cycle at pseudo-steady state, corresponding to day 157 in R1 (a), and day 199 in R2 (b).

cycle and consumed simultaneously with the production of PHA. During this phase, no significant cell growth was observed, mostly due to the nitrogen source only being fed after the exhaustion of the carbon source. During the famine phase, the intracellularly stored PHA and the soluble ammonia were consumed concomitantly, resulting in biomass growth.

Table 1 presents the average and standard deviation of kinetic and stoichiometric parameters calculated in the feast phases for both reactors during pseudo-steady state operation. A slightly higher yield of PHA produced per substrate consumed was observed in R1 (0.59 ± 0.1 Cmol-PHA.Cmol-S^{-1}) than in R2 (0.44 ± 0.2 Cmol-PHA.Cmol-S^{-1}), but the difference was not statistically significant within a confidence interval of 95 %. The specific PHA production rates observed in R1 and R2 (0.44 ± 0.09 Cmol-PHA.Cmol-X_A^{-1}.h^{-1} vs 0.36 ± 0.09 Cmol-PHA.Cmol-X_A^{-1}.h^{-1}, respectively), and the specific substrate consumption rates (0.63 ± 0.08 Cmol-PHA.Cmol-X_A^{-1}.h^{-1} for R1 vs 0.73 ± 0.1 Cmol-S.Cmol-X_A^{-1}.h^{-1} for R2) were not statistically significant at a significance level of 0.05. Another important factor is the maximum PHA content reached during the feast phase. As presented in Table 1, biomass in R2 stored up to 32.7 ± 5.3 wt.% PHA during the feast phase, while biomass from R1 stored only 19.3 ± 7.7 wt.% PHA. The PHA content per cell was higher in R2 because the concentration of active biomass in R1 was about 3.4 times higher than R2 (2.8 ± 0.4 g-X_A.L^{-1} and 0.83 ± 0.2 g-X_A.L^{-1}, respectively), resulting in a higher availability of substrate per cell for R2 that can be stored as PHA. As expected, the volumetric PHA production rate during the feast phase was much higher in R1 (0.89 ± 0.3 g-PHA.L^{-1}.h^{-1}) than in R2 (0.25 ± 0.06 g-PHA.L^{-1}.h^{-1}), due to the higher biomass concentration. Overall, the results indicate that both cultures have similar specific capacities per cell to accumulate PHA, but the higher biomass concentration of R1 results in a higher volumetric PHA production rate.

Table 1
Feast phase-related stoichiometric and kinetic parameters in selection reactors R1 and R2. The values presented are mean ± standard deviation from cycles (n = 6) assessed during a period of pseudo-steady state.

Feast phase	R1	R2
F/F (h. h^{-1})	0.08 ± 0.03	0.24 ± 0.1
$-q_S$ (Cmol-S.Cmol-X_A^{-1}.h^{-1})	0.63 ± 0.08	0.73 ± 0.1
q_{PHA} (Cmol-PHA.Cmol-X_A^{-1}.h^{-1})	0.44 ± 0.09	0.36 ± 0.09
$Y_{PHA/S}$ (Cmol-PHA.Cmol-S^{-1})	0.59 ± 0.1	0.44 ± 0.2
PHA^{max} (wt.%)	19.3 ± 7.7	32.7 ± 5.3
r_{PHA} (g-PHA.L^{-1}.h^{-1})	0.89 ± 0.3	0.25 ± 0.06

Table 2 shows parameters related to the famine phase of both reactors. R1 produced (ΔX) on average a higher amount of biomass per cycle (0.91 ± 0.2 g-X_A) than R2 (0.55 ± 0.1 g-X_A), agreeing well with the difference in steady state biomass concentration of each reactor. The constant k and $Y_{X/PHA}$ were found to be similar between both reactors (Table 2) and comparable to those described in the literature. The values of k calculated in this study, 0.12 ± 0.04 Cmol-$PHA^{1/3}$.Cmol-$X_A^{-1/3}$.h^{-1} for R1 and 0.15 ± 0.007 Cmol-$PHA^{1/3}$.Cmol-$X_A^{-1/3}$.h^{-1} for R2, were similar to those calculated by [34] for a cycle length of 12 h (0.15 – 0.25 Cmol-$PHA^{1/3}$.Cmol-$X_A^{-1/3}$.h^{-1}). Since k is related to the specific rate of PHA degradation, these results indicate that the cultures selected had similar capacity to metabolize the cell internal reserves of PHA.

R1 had a higher biomass productivity (0.82 ± 0.08 g-X_A.L^{-1}.d^{-1}) than R2 (0.21 ± 0.05 g-X_A.L^{-1}.d^{-1}). The only operational difference between the reactors studied was the timing of biomass withdrawal. In R2, 12.5 % of the volume of biomass was removed per cycle from the reactor at the end of the feast phase, corresponding to a decrease in the amount of biomass subjected to the presence of nutrients that allow growth during the famine phase, unlike R1. Thus, the difference in biomass concentration between both cultures was likely to be due to the higher fraction of biomass from SBR1 that could grow during the famine phase, which clearly had a cumulative impact on the biomass concentration in each SBR over time.

Population analysis by high-throughput sequencing

The microbial cultures selected in both reactors were analysed by high-throughput sequencing of the 16S V1-3 rRNA gene. The initial seed sludge presented 37 different genera identified at a relative abundance of >0.1 %, consistent with that expected from non-selected activated sludge. The relative abundance of microorganisms identified in samples from R1 (day 157) and R2 (day 199) during a period of steady state operation is presented in Table 3. The two most abundant genera in both SBRs were *Neomegalonema* (formerly known as *Meganema*) and *Xanthobacter*, however, while *Xanthobacter* was dominant in R1 (52.9 %), *Neomegalonema* was dominant in R2 (88.0 %). A high abundance of genera often reported to include PHA-storing species were identified in both reactors in different relative abundances, including *Neomegalonema*, *Xanthobacter, Leucobacter, Leadbetterella, Thiothrix, Paracocccus, Luteimonas, Brevundimonas, Chelatococcus, Amaricoccus, Rhodobacter* and *Stenotrophomonas* [9,11,18,26,35,36]. Moreover, microorganisms from genera *Leucobacter, Luteimonas, Chelatococcus*, *Rhodobacter* and *Stenotrophomonas* were also identified in R1 (8.9 %), and *Thiothrix* was present in R2 (1.7 %). The results obtained were consistent

Table 2
Famine phase-related stoichiometric and kinetic parameters in selection reactors R1 and R2. The values presented are mean ± standard deviation from cycles (R1: n = 5 and R2: n = 3) of a period of pseudo-steady state.

Famine phase	R1	R2
ΔX (g-X_A)	0.91 ± 0.2	0.55 ± 0.1
k (Cmol-$PHA^{1/3}$.Cmol-$X_A^{-1/3}$. h^{-1})	0.12 ± 0.04	0.15 ± 0.007
$Y_{X/PHA}$ (Cmol-X.Cmol-PHA^{-1})	0.80 ± 0.2	0.86 ± 0.01
$Prod_X$ (g-X_A.L^{-1}.d^{-1})	0.82 ± 0.08	0.21 ± 0.05

Table 3
Relative abundance (>0.1 %) of bacteria identified by high-throughput sequencing in the two SBRs under a stable period of operation. Genera in bold text contain species known to exhibit PHA production potential.

R1			R2		
Class	Genus	%	Class	Genus	%
Alphaproteobacteria	***Xanthobacter***	**52.94**	*Alphaproteobacteria*	***Neomegalonema***	**87.96**
Alphaproteobacteria	***Neomegalonema***	**8.05**	*Alphaproteobacteria*	***Xanthobacter***	**5.02**
Actinobacteria	***Leucobacter***	**7.32**	*Gammaproteobacteria*	***Thiothrix***	**1.66**
	*SHA-109**	7.26	*Alphaproteobacteria*	*Rhodobacteraceae****	0.66
Alphaproteobacteria	*Rhodobacteraceae****	5.47	*Alphaproteobacteria*	***Amaricoccus***	**0.65**
Flavobacteria	***Leadbetterella***	**2.78**	*Alphaproteobacteria*	***Paracocccus***	**0.58**
Gammaproteobacteria	*Pseudoxanthomonas*	2.22	*Flavobacteria*	*Chryseobacterium*	0.41
Alphaproteobacteria	*Mesorhizobium*	1.61	*Gammaproteobacteria*	*Pseudoxanthomonas*	0.31
Alphaproteobacteria	*Devosia*	1.57	*Alphaproteobacteria*	***Brevundimonas***	**0.26**
Alphaproteobacteria	***Paracocccus***	**1.18**	*Flavobacteria*	***Leadbetterella***	**0.17**
Alphaproteobacteria	*Stappia*	0.94	*Alphaproteobacteria*	*Devosia*	0.14
Gammaproteobacteria	*Arenimonas*	0.90			
Gammaproteobacteria	***Luteimonas***	**0.69**			
Alphaproteobacteria	***Brevundimonas***	**0.52**			
Alphaproteobacteria	***Chelatococcus***	**0.43**			
Alphaproteobacteria	*Rhizobium*	0.39			
Alphaproteobacteria	***Amaricoccus***	**0.34**			
Alphaproteobacteria	*Rhizobiales***	0.29			
Alphaproteobacteria	***Rhodobacter***	**0.29**			
Gammaproteobacteria	***Stenotrophomonas***	**0.18**			

* Identified only to the phylum level.
** Identified only to the order level.
*** Identified only to the family level.

with the observations made by microscopy (Fig. 2). R2 was dominated by filamentous bacteria, consistent with *Neomegalonema* and *Thiothrix*, and both reactors revealed a large number of PHA granules from Nile Blue staining (Fig. 2). In addition, an undisclosed OTU from phylum SHA-109 and an unidentified member of the family *Rhodobacteraceae* were also present in high relative abundance in R1. Overall, the sequencing results suggest that the culture was highly enriched in PHA-storing organisms, supporting the idea that both reactors were effective in selecting PHA accumulating organisms. It was also clear that the dominant genera were different due to the different growth conditions associated with withdrawing biomass from the reactors at the end of either the feast or famine phase. Also, the difference in microbial composition could have impacted on the storage response of the biomass.

Accumulation assays

Accumulation assays (referred to as R1-Ac and R2-Ac when using biomass from R1 and R2, respectively) were performed to evaluate the maximum PHA accumulation capacity of the microbial cultures selected. The PHA content profile (wt.%) of R1-Ac and R2-Ac is presented in Fig. 3 (I-A and II-A), corresponding to two replicate accumulation assays (Ac1 and Ac2) for each reactor, as well as the VSS concentration and amount of VFA over time (I-B and II-B). It should be noted that the initial PHA content of R2-Ac (Fig. 3, II-A) was much higher than that of R1-Ac (Fig. 3, I-A), since the biomass used in the accumulation assays was removed from R2 at the end of the feast phase, while it was removed from R1 at the end of the famine phase. The maximum PHA content accumulated by both cultures was similar for R1-Ac and R2-Ac (51.7 ± 1.5 wt.% vs 56.1 ± 1.0 wt.% respectively), but corresponded to 3.5 ± 0.3 g-PHA.L^{-1} obtained from the selected biomass from R1 and 2.2 ± 0.02 g-PHA.L^{-1} from R2, considering that the accumulation assays for both reactors had different initial biomass concentrations (3.7 ± 0.6 g-VSS.L^{-1} for R1-Ac vs 2.0 ± 0.3 g-VSS.L^{-1} for R2-Ac) and different volumes of carbon source solution added (Fig. 3, I-B and II-B).

Despite the different biomass withdrawal strategies applied to the selection reactors, Table 4 shows that the performance of both cultures was very similar, with maximum specific substrate consumption rates of 0.53 ± 0.04 Cmol-S.Cmol-$X_A{}^{-1}$.h^{-1} and 0.52 ± 0.1 Cmol-S.Cmol-$X_A{}^{-1}$.

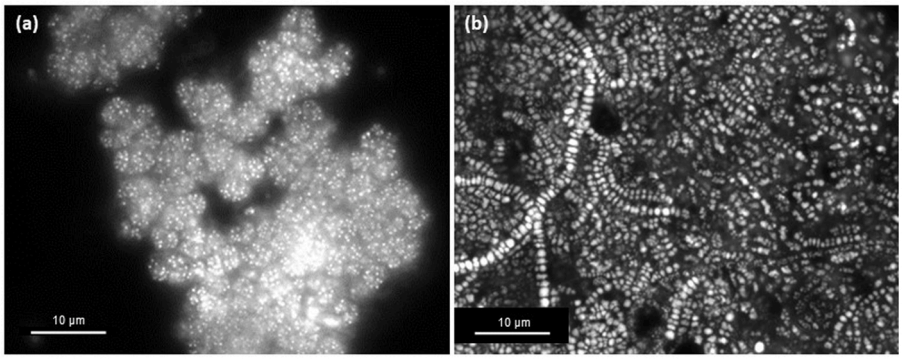

Fig. 2. Fluorescence microscopy images of fresh biomass samples after Nile blue staining collected at the end of the feast phase during a cycle monitorization performed in R1 (day 157, a) and R2 (day 192, b). The white dots correspond to the intracellular inclusions of PHA.

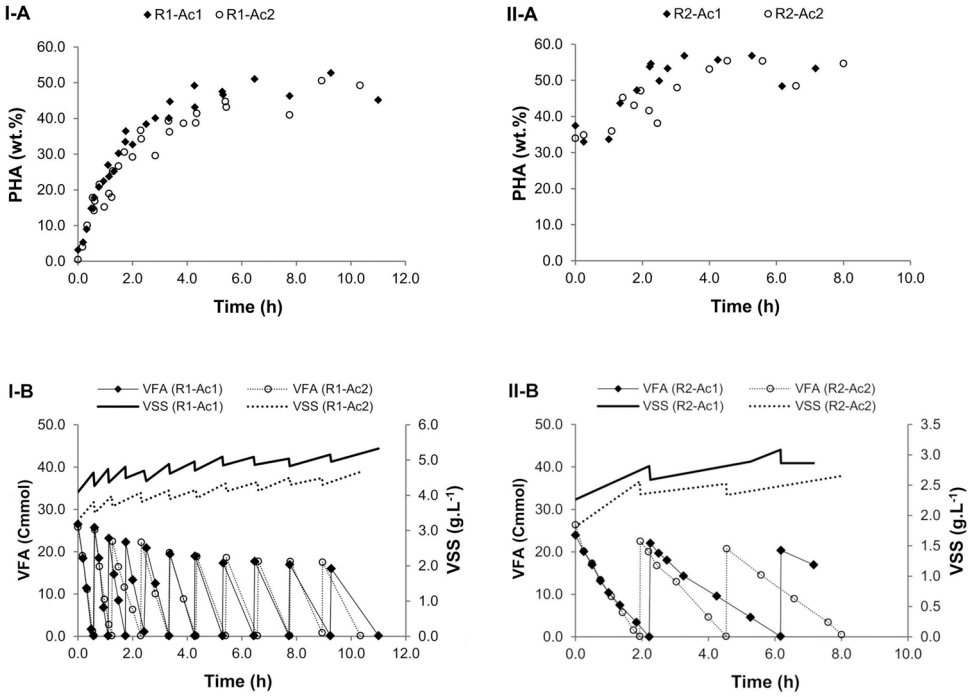

Fig. 3. Overall results of the accumulation assays (Ac1 and Ac2 are replicates) performed using biomass from R1 (I-A and I-B) and R2 (II-A and II-B), showing the % PHA, the VSS concentration and the amount of VFA over time. The maximum values of VFA correspond to the addition of feed pulses.

Table 4
Performance parameters of the PHA accumulation assays performed with biomass selected from R1 and R2. The values presented are mean ± standard deviation from the replicates performed.

Reactor	R1-Ac	R2-Ac
X_A (Cmmol), average	62.5 ± 6.2	20.6 ± 0.4
Maximum biomass activity		
$-q_S^{max}$ (Cmol-S.Cmol-X_A^{-1}. h^{-1})	0.53 ± 0.04 [a]	0.52 ± 0.1 [b]
q_{PHA}^{max} (Cmol-PHA.Cmol-X_A^{-1}. h^{-1})	0.38 ± 0.07 [a]	0.44 ± 0.03 [b]
$Y_{PHA/S}^{max}$ (Cmol-PHA.Cmol-S^{-1})	0.78 ± 0.07 [a]	0.82 ± 0.2 [b]
r_{PHA}^{max} (g-PHA.L^{-1}. h^{-1})	0.97 ± 0.2 [a]	0.39 ± 0.04 [b]
Overall accumulation performance*		
Elapsed time (h)	6.6 ± 1.1	4.4 ± 1.2
PHA^{max}(wt.%)	51.7 ± 1.5	56.1 ± 1.0
HV (Cmol%)	19.1 ± 3.3	44.9 ± 3.3
$Y_{PHA/S}$ (Cmol-PHA.Cmol-S^{-1})	0.63 ± 0.05	0.64 ± 0.1
r_{PHA} (g-PHA.L^{-1}. h^{-1})	0.49 ± 0.1	0.24 ± 0.03

[a] average of the first 3 pulses.
[b] calculated for the first pulse.
* The authors defined a threshold of 90 % of the maximum capacity of the culture to produce PHA in order to normalize the results obtained in all the accumulation assays performed. All calculations are described in Section 2.5.

h^{-1} for R1-Ac and R2-Ac, respectively, and maximum specific PHA production rates of 0.38 ± 0.07 Cmol-PHA.Cmol-X_A^{-1}.h^{-1} and 0.44 ± 0.03 Cmol-PHA.Cmol-X_A^{-1}.h^{-1}, which are not significantly different at a confidence interval of 95 %. Consequently, the yield of PHA obtained in the first 2 h of the accumulation assays (period of maximum biomass activity) was very similar between R1-Ac and R2-Ac, corresponding to 0.78 ± 0.07 Cmol-PHA.Cmol-S^{-1} and 0.82 ± 0.2 Cmol-PHA.Cmol-S^{-1}, respectively. It should be noted that the biomass from R1 and R2 that was inoculated into the PHA production reactors came from very different physiological states. Biomass purged from R1 had been submitted to a long starvation period during the famine phase (growth and maintenance were the main processes occurring), while biomass purged from R2 corresponded to biomass performing the uptake of substrate and storage of PHA during the feast phase of the selection reactor. However, accumulations assays performed for both cultures presented similar initial specific substrate uptake and PHA production rates ($-q_S^{max}$, q_{PHA}^{max}, Table 4), indicating that the physiological state of the biomass did not affect its capacity to store PHA during the PHA accumulation stage.

As the accumulation assay progressed, and the cells became enriched with PHA granules, the specific PHA production rate and the capacity of biomass to produce PHA both decreased substantially, as expected and observed by others [9,20,25,37], reaching a plateau which corresponds to its maximum PHA accumulation capacity (Fig. 3). The overall yield was similar for the accumulation assays performed, corresponding to 0.63 ± 0.05 Cmol-PHA.Cmol-S^{-1} for R1-Ac and 0.64 ± 0.1 Cmol-PHA.Cmol-S^{-1} for R2-Ac. The volumetric PHA production rate in R1 tests was significantly higher than in R2 tests (Table 4) due to the higher biomass concentration of R1.

The PHA monomeric composition (3HB:3HV) is a determining factor for possible polymer applications. Here, significantly different PHA compositions were obtained, with R1 producing a polymer with 19.1 ± 3.3 %Cmol 3HV monomers and R2 one with 44.9 ± 3.3 %Cmol 3HV (Table 4). Given that the feed composition was the same for both reactors, this disparity could be explained by the different microbial populations enriched in the two selection reactors, in agreement with the results obtained by [38], where it was found that the 3HV content of the polymer was strongly correlated with the composition of the microbial population. R1 and R2 have different dominant genera, *Xanthobacter and Neomegalonema*, respectively, which may employ different metabolic pathways, such as the production of 3HV either from acetate and propionate or from propionate alone, leading to different proportions of 3HB and 3HV monomers. Copolymers with considerably different 3HV contents have different physicochemical properties (e.g, melting temperature, crystallization, Young's modulus); while

copolymers with around 20 %Cmol 3HV are considered to be most suitable for the production of food packaging (gas barrier properties), a higher 3HV monomer content results in softer and more elastic copolymers with alternative applications such as adhesives and elastomeric films [39,40]. Thus, the biomass withdrawal strategy can be used to select a culture that produces a copolymer enriched in 3HV monomers.

Perspectives on the advantages of different biomass withdrawal strategies in integrated PHA production processes by MMC

The global PHA productivity, considering the contributions of both the selection reactor and the accumulation reactor, was calculated in order to compare both systems. R1 had a global PHA productivity approximately twice that of R2, namely 1.6 ± 0.3 g-PHA.L^{-1}.d^{-1} vs 0.73 ± 0.3 g-PHA.L^{-1}.d^{-1}. The major contributing factor for this difference was the volumetric biomass productivity, which was much higher in R1 than in R2 (0.82 ± 0.08 g-X_A.L^{-1}.d^{-1} vs 0.21 ± 0.05 g-X_A.L^{-1}.d^{-1}). The advantage of R2 was the shorter time required for PHA accumulation (Table 4), which supports the implementation of a smaller accumulation reactor and associated savings in capital costs when translated to a continuously operated full-scale PHA production facility. The scenario was also considered in which the biomass from the selection reactor of R2 was immediately directed towards downstream processing, since the biomass withdrawal strategy of R2 could potentially lead to the elimination of the accumulator reactor. However, in this case, PHA productivity of the selection reactor, considering the volumetric biomass productivity and the specific PHA concentration at the end of the feast phase, was severely reduced, resulting in 0.10 ± 0.04 g-PHA.L^{-1}.d^{-1} being achieved when by-passing the accumulation stage.

The global PHA productivity values underline the importance of the volumetric biomass productivity in the process of PHA production. Since significantly more biomass was produced in the selection reactor R1, more purged biomass was available to perform the accumulation assays and, even if the maximum PHA content was similar in both accumulators, the R1 accumulation assays were able to produce a considerably higher amount of PHA than those of R2.

Others operated a system similar to the R2 here, in terms of carbon source and an uncoupled C-N feeding strategy, but with higher OLR (4.25 g-COD.L^{-1}.d^{-1}, equivalent to 127 Cmmol.L^{-1}.d^{-1}, vs 100 Cmmol.L^{-1}.d^{-1} used here) and lower SRT (1 day vs 4 days here), and obtained a global PHA productivity of 2.24 ± 0.06 g-PHA.L^{-1}.d^{-1} [20]. Furthermore, when the OLR increased from 4.25 to 8.5 g-COD.L^{-1}.d^{-1}, PHA productivity increased to 2.89 ± 0.05 g-PHA.L^{-1}.d^{-1} [20]. Although the study of [20] cannot be directly compared to the present work, since the SRT was significantly lower than that imposed here, the results suggest that tuning the operational conditions may improve the performance of R2. Thus, optimizing operational conditions such as the OLR and/or the SRT for different biomass withdrawal strategies should be studied in order to evaluate the resulting impact on the competitiveness of each strategy. Ideally, if the PHA content and PHA productivity could be maximized directly in the selection reactor, PHA-rich biomass could be removed at the end of the feast phase and moved directly to downstream processing and PHA recovery steps, avoiding the accumulation stage and significantly reducing equipment and energetic costs [41]. Nevertheless, as this study shows, the decrease in biomass productivity can potentially outweigh this advantage, leading to lower overall PHA productivity, as observed under the studied operational scenario.

Conclusions

This study has assessed for the first time the impact of biomass withdrawal strategy on PHA productivity by MMC, which was compared in parallel SBRs. It demonstrated that both systems selected cultures with similar capacity for PHA production, but that removing the excess biomass at the end of the feast phase resulted in lower global volumetric biomass productivity. This was the key parameter affecting the global PHA productivity of the 2-stage system. Our results support the approach of withdrawing biomass at the end of the famine phase as a means of optimizing PHA productivity. However, further evaluation of the impact of a biomass withdrawal strategy at different organic loading rates and solids retention times is warranted in order to compare the joint effect of these operational parameters in unison.

Acknowledgements

This research was financed by national funds from FCT – Fundação para a Ciência e a Tecnologia, I.P., in the scope of the project UIDP/04378/2020 and UIDB/04378/2020 of the Research Unit on Applied Molecular Biosciences – UCIBIO and the project LA/P/0140/2020 of the Associate Laboratory Institute for Health and Bioeconomy – I4HB. Rafaela Cruz also acknowledges FCT for the financial support through the Ph.D. Grant SFRH/BD/110673/2015. The authors further acknowledge Elsa Mora, Mónica Centeio and Elisabete Freitas for their contribution with quantitative analysis and Elisabete Freitas for help with microbiology samples.

Appendix A. Supplementary data

Supplementary material related to this article can be found, in the online version, at doi:https://doi.org/10.1016/j.nbt.2021.08.004.

References

[1] Verlinden RAJJ, Hill DJ, Kenward MA, Williams CD, Radecka I. Bacterial synthesis of biodegradable polyhydroxyalkanoates. J Appl Microbiol 2007;102:1437–49. https://doi.org/10.1111/j.1365-2672.2007.03335.x.

[2] Crank M, Patel M, Marscheider-Weidemann F, Schleich J, Hüsing B, Angerer G. Techno-economic feasibility of large-scale production of bio-based polymers in Europe (PRO-BIP); Final Report (NWS-E–2004-2111). The Netherlands. 2005. https://inis.iaea.org/search/searchsinglerecord.aspx?recordsFor=SingleRecord&RN=37032239.

[3] Dias JML, Lemos PC, Serafim LS, Oliveira C, Eiroa M, Albuquerque MGE, et al. Recent advances in polyhydroxyalkanoate production by mixed aerobic cultures: from the substrate to the final product. Macromol Biosci 2006;6:885–906. https://doi.org/10.1002/mabi.200600112.

[4] Reis MAM, Serafim LS, Lemos PC, Ramos AM, Aguiar FR. Van Loosdrecht MCM. Production of polyhydroxyalkanoates by mixed microbial cultures. Bioprocess Biosyst Eng 2003;25:377–85. https://doi.org/10.1007/s00449-003-0322-4.

[5] Albuquerque MGE, Torres CAV, Reis MAM. Polyhydroxyalkanoate (PHA) production by a mixed microbial culture using sugar molasses: effect of the influent substrate concentration on culture selection. Water Res 2010;44:3419–33. https://doi.org/10.1016/j.watres.2010.03.021.

[6] Oliveira CSS, Silva CE, Carvalho G, Reis MA. Strategies for efficiently selecting PHA producing mixed microbial cultures using complex feedstocks: feast and famine regime and uncoupled carbon and nitrogen availabilities. N Biotechnol 2017;37:69–79. https://doi.org/10.1016/j.nbt.2016.10.008.

[7] Dionisi D, Carucci G, Papini MP, Riccardi C, Majone M, Carrasco F, et al. Olive oil mill effluents as a feedstock for production of biodegradable polymers. Water Res 2005;39:2076–84. https://doi.org/10.1016/j.watres.2005.03.011.

[8] Salmiati ZU, Salim MR, Md Din MF, Ahmad MA. Intracellular biopolymer productions using mixed microbial cultures from fermented POME. Water Sci Technol 2007;56:179–85. https://doi.org/10.2166/wst.2007.687.

[9] Tamis J, Lužkov K, Jiang Y, Loosdrecht MCM van, Kleerebezem R. Enrichment of Plasticicumulans acidivorans at pilot-scale for PHA production on industrial wastewater. J Biotechnol 2014;192:161–9. https://doi.org/10.1016/j.jbiotec.2014.10.022.

[10] Bengtsson S, Werker A, Christensson M, Welander T. Production of polyhydroxyalkanoates by activated sludge treating a paper mill wastewater. Bioresour Technol 2008;99:509–16. https://doi.org/10.1016/j.biortech.2007.01.020.

[11] Jiang Y, Chen Y, Zheng X. Efficient polyhydroxyalkanoates production from a waste-activated sludge alkaline fermentation liquid by activated sludge submitted to the aerobic feeding and discharge process. Environ Sci Technol 2009;43:7734–41. https://doi.org/10.1021/es9014458.

[12] Korkakaki E, Mulders M, Veeken A, Rozendal R, van Loosdrecht MCM, Kleerebezem R. PHA production from the organic fraction of municipal solid waste (OFMSW): overcoming the inhibitory matrix. Water Res 2016;96:74–83. https://doi.org/10.1016/j.watres.2016.03.033.

[13] Moretto G, Russo I, Bolzonella D, Pavan P, Majone M, Valentino F. An urban biorefinery for food waste and biological sludge conversion into polyhydroxyalkanoates and biogas. Water Res 2020;170:115371. https://doi.org/10.1016/j.watres.2019.115371.

[14] Stegmann P, Londo M, Junginger M. The circular bioeconomy: its elements and role in European bioeconomy clusters. Resour Conserv Recycl X 2020;6:100029. https://doi.org/10.1016/j.rcrx.2019.100029.
[15] Karan H, Funk C, Grabert M, Oey M, Hankamer B. Green Bioplastics as part of a circular bioeconomy. Trends Plant Sci 2019;24:237–49. https://doi.org/10.1016/j.tplants.2018.11.010.
[16] Albuquerque MGE, Eiroa M, Torres C, Nunes BR, Reis MAM. Strategies for the development of a side stream process for polyhydroxyalkanoate (PHA) production from sugar cane molasses. J Biotechnol 2007;130:411–21. https://doi.org/10.1016/j.jbiotec.2007.05.011.
[17] Dionisi D, Majone M, Papa V, Beccari M. Biodegradable polymers from organic acids by using activated sludge enriched by aerobic periodic feeding. Biotechnol Bioeng 2004;85:569–79. https://doi.org/10.1002/bit.10910.
[18] Coats ER, Watson BS, Brinkman CK. Polyhydroxyalkanoate synthesis by mixed microbial consortia cultured on fermented dairy manure: effect of aeration on process rates/yields and the associated microbial ecology. Water Res 2016;106:26–40. https://doi.org/10.1016/j.watres.2016.09.039.
[19] Valentino F, Morgan-Sagastume F, Campanari S, Villano M, Werker A, Majone M. Carbon recovery from wastewater through bioconversion into biodegradable polymers. N Biotechnol 2017;37. https://doi.org/10.1016/j.nbt.2016.05.007.
[20] Lorini L, di Re F, Majone M, Valentino F. High rate selection of PHA accumulating mixed cultures in sequencing batch reactors with uncoupled carbon and nitrogen feeding. N Biotechnol 2020;56:140–8. https://doi.org/10.1016/j.nbt.2020.01.006.
[21] Silva F, Campanari S, Matteo S, Valentino F, Majone M, Villano M. Impact of nitrogen feeding regulation on polyhydroxyalkanoates production by mixed microbial cultures. N Biotechnol 2017;37:90–8. https://doi.org/10.1016/j.nbt.2016.07.013.
[22] Campanari S, Augelletti F, Rossetti S, Sciubba F, Villano M, Majone M. Enhancing a multi-stage process for olive oil mill wastewater valorization towards polyhydroxyalkanoates and biogas production. Chem Eng J 2017;317:280–9. https://doi.org/10.1016/j.cej.2017.02.094.
[23] Reis M, Albuquerque M, Villano M, Majone M. Mixed culture processes for polyhydroxyalkanoate production from agro-industrial Surplus/Wastes as feedstocks. second edi, vol. 6. Elsevier B.V.; 2011. https://doi.org/10.1016/B978-0-08-088504-9.00464-5.
[24] Campanari S, E Silva FA, Bertin L, Villano M, Majone M. Effect of the organic loading rate on the production of polyhydroxyalkanoates in a multi-stage process aimed at the valorization of olive oil mill wastewater. Int J Biol Macromol 2014;71:34–41. https://doi.org/10.1016/j.ijbiomac.2014.06.006.
[25] Johnson K, Jiang Y, Kleerebezem R, Muyzer G, van Loosdrecht MCM. Enrichment of a mixed bacterial culture with a high polyhydroxyalkanoate storage capacity. Biomacromolecules 2009;10:670–6. https://doi.org/10.1021/bm8013796.
[26] Wang X, Oehmen A, Freitas EB, Carvalho G, Reis MAM. The link of feast-phase dissolved oxygen (DO) with substrate competition and microbial selection in PHA production. Water Res 2017;112:269–78. https://doi.org/10.1016/j.watres.2017.01.064.
[27] Irvine RL, Busch AW. Sequencing batch biological reactors: an overview. J Water Pollut Control Fed 1979;51:235–43. http://www.jstor.org/stable/25039819.
[28] Serafim LS, Lemos PC, Oliveira R, Reis MAM. Optimization of polyhydroxybutyrate production by mixed cultures submitted to aerobic dynamic feeding conditions. Biotechnol Bioeng 2004;87:145–60. https://doi.org/10.1002/bit.20085.
[29] Albuquerque MGE, Martino V, Pollet E, Avérous L, Reis MAM. Mixed culture polyhydroxyalkanoate (PHA) production from volatile fatty acid (VFA)-rich streams: effect of substrate composition and feeding regime on (PHA) productivity, composition and properties. J Biotechnol 2011;151:66–76. https://doi.org/10.1016/j.jbiotec.2010.10.070.
[30] Lorini L, Martinelli A, Pavan P, Majone M, Valentino F. Downstream processing and characterization of polyhydroxyalkanoates (PHAs) produced by mixed microbial culture (MMC) and organic urban waste as substrate. Biomass Convers Biorefinery 2020. https://doi.org/10.1007/s13399-020-00788-w.
[31] APHA. Standard methods for the examination of water and wastewater. Washington DC. 1999. https://www.standardmethods.org/.
[32] Lanham AB, Ricardo AR, Albuquerque MGEE, Pardelha F, Carvalheira M, Coma M, et al. Determination of the extraction kinetics for the quantification of polyhydroxyalkanoate monomers in mixed microbial systems. Process Biochem 2013;48:1626–34. https://doi.org/10.1016/j.procbio.2013.07.023.
[33] Caporaso JG, Lauber CL, Walters WA, Berg-Lyons D, Huntley J, Fierer N, et al. Ultra-high-throughput microbial community analysis on the Illumina HiSeq and MiSeq platforms. ISME J 2012;6:1621–4. https://doi.org/10.1038/ismej.2012.8.
[34] Tamis J, Marang L, Jiang Y, van Loosdrecht MCMM, Kleerebezem R. Modeling PHA-producing microbial enrichment cultures-towards a generalized model with predictive power. N Biotechnol 2014;31:324–34. https://doi.org/10.1016/j.nbt.2013.11.007.
[35] Cui B, Huang S, Xu F, Zhang R, Zhang Y. Improved productivity of poly (3-hydroxybutyrate) (PHB) in thermophilic Chelatococcus daeguensis TAD1 using glycerol as the growth substrate in a fed-batch culture. Appl Microbiol Biotechnol 2015;99:6009–19. https://doi.org/10.1007/s00253-015-6489-1.
[36] Iqbal B, Khan N, Jamil N. Polyhydroxybutyrate production by Stenotrophomonas and Exiguobacterium using renewable carbon source. Annu Res Rev Biol 2016;9:1–9. https://doi.org/10.9734/ARRB/2016/23066.
[37] Jiang Y, Marang L, Kleerebezem R, Muyzer G, van Loosdrecht MCM. Polyhydroxybutyrate production from lactate using a mixed microbial culture. Biotechnol Bioeng 2011;108:2022–35. https://doi.org/10.1002/bit.23148.
[38] Carvalho G, Oehmen A, Albuquerque MGE, Reis MAM. The relationship between mixed microbial culture composition and PHA production performance from fermented molasses. N Biotechnol 2014;31:257–63. https://doi.org/10.1016/j.nbt.2013.08.010.
[39] Arcos-Hernández MV, Laycock B, Donose BC, Pratt S, Halley P, Al-Luaibi S, et al. Physicochemical and mechanical properties of mixed culture polyhydroxyalkanoate (PHBV). Eur Polym J 2013;49:904–13. https://doi.org/10.1016/j.eurpolymj.2012.10.025.
[40] Philip S, Keshavarz T, Roy I. Polyhydroxyalkanoates: biodegradable polymers with a range of applications. J Chem Technol Biotechnol 2007;82:233–47. https://doi.org/10.1002/jctb.1667.
[41] Valentino F, Beccari M, Fraraccio S, Zanaroli G, Majone M. Feed frequency in a Sequencing Batch Reactor strongly affects the production of polyhydroxyalkanoates (PHAs) from volatile fatty acids. N Biotechnol 2014;31. https://doi.org/10.1016/j.nbt.2013.10.006.